SEBHA UNIVERSITY CONFERENCE PROCEEDINGS, VOL.5 NO. 4 2026
DOI: 10.51984/3N53HY31

وقائع مؤتمرات جامعة سبها
Sebha University Conference Proceedings
Confrence Proceeeding homepage: http://www.sebhau.edu.ly/journal/CAS

Hybrid Adaptive Anti-Windup PID Control for UAV Altitude Regulation Under Actuator Saturation: A Monte Carlo and Statistical Performance Evaluation

Montaser Ali Saeed [a*], Tarik Hassan Elsonni [b], Souzan S. Abdulhafith [a], Kamala Abdulhafith [a], Ahmed Belmashkan [a], Mohamed Fathi [a]

[a]Aeronautical Engineering Department, Faculty of Aeronautics, Bright Star University, El Brega, Libya
[b]Department of Aeronautical Engineering, Faculty of Engineering, Sudan University of Science and Technology, Khartoum, Sudan

Keywords:
Adaptive Control
Anti-Windup Compensation
PID Controller
Actuator Saturation
Uncrewed Aerial Vehicles (UAVs)
Lyapunov-Based Convergence Analysis

ABSTRACT

This study develops a Hybrid Adaptive Anti-Windup PID controller for altitude regulation of a three-degree-of-freedom (3-DOF) Uncrewed Aerial Vehicle (UAV) operating under actuator saturation constraints. The proposed architecture continuously adjusts the anti-windup compensation based on the instantaneous severity of actuator limiting via a saturation-dependent adaptive weighting mechanism. The controller is evaluated against No Anti-Windup, Back-Calculation, and Conditional Integration strategies using Monte Carlo simulations comprising 50 independent runs for each of six challenging operating scenarios, including wind disturbances, payload variations, increased aerodynamic drag, large reference commands, and combined disturbances. Performance is assessed using Integral Absolute Error (IAE), overshoot, settling time, actuator saturation, and statistical measures. Across the evaluated scenarios, the Hybrid Adaptive strategy achieves IAE reductions of 58–65%, overshoot reductions of 80–88%, actuator-saturation reductions of 50–60%, and settling-time reductions of 28–35% relative to the No Anti-Windup baseline. The corresponding average reductions are 61.5%, 83.8%, 55.2%, and 30.7%, respectively. Analysis of variance (ANOVA) indicates statistically significant differences among the evaluated control strategies for all scenarios ((p<0.001)). At the same time, eta-squared effect sizes range from 0.58 to 0.75, with an overall mean of 0.68, indicating substantial practical effects. A Lyapunov-based convergence analysis is also formulated to provide a theoretical assessment of the closed-loop behavior under actuator constraints. The results further demonstrate effective altitude regulation under wind disturbances and positive actuator margins across the tested operating conditions. However, performance becomes more demanding under increased payload and reduced control authority. Overall, the findings indicate that saturation-dependent anti-windup compensation can improve tracking accuracy, transient recovery, disturbance rejection, and actuator utilization while retaining a relatively simple PID-based control structure. Future work will address experimental validation, parameter-sensitivity analysis, comparison with modern constrained-control approaches, and extension to a full 6-DOF UAV model.

متحكم PID هجين تكيفي مضاد لتشبع المتكامل للتحكم في ارتفاع الطائرات غير المأهولة تحت قيود تشبع المشغلات: تقييم بالأُسلوب الإحصائي ومحاكاة مونت كارلو

منتصر علي سعيد محمد[a] ؛ طارق حسن السني[b]؛ سوزان عبد الحفيظ[a]؛ كاملة عبد الحفيظ[a]؛ احمد بالمشكان[a]؛محمد فتحي العريبي[a]

[a] قسم هندسة الطيران، كلية علوم الطيران، جامعة النجم الساطع، البريقة، ليبيا
[b] قسم هندسة الطيران، كلية الهندسة، جامعة السودان للعلوم والتكنولوجيا، الخرطوم، السودان

الكلمات المفتاحية:
التحكمPID
مقاومة تشبع المشغلات
التحكم التكيفي
الطائرات غير المأهولة
تحليل التقارب
تحليل التباين الإحصائي.

الملخص

تقدم هذه الدراسة متحكم PID هجينًا تكيفيًا مزودًا بآلية مضادة لتراكم التكامل لتنظيم ارتفاع طائرة غير مأهولة ذات ثلاث درجات حرية (3-DOF UAV) تعمل في ظل قيود تشبع المشغلات. تعتمد البنية المقترحة على تعديل تعويض مقاومة تراكم التكامل بصورة مستمرة وفق شدة تقييد المشغل في اللحظة الراهنة، وذلك من خلال آلية وزن تكيفية مرتبطة بدرجة التشبع. جرى تقييم المتحكم ومقارنته باستراتيجيات عدم استخدام مقاومة تراكم التكامل، والتعويض بالتغذية الراجعة العكسية(Back-Calculation) ، والتكامل الشرطي (Conditional Integration)، باستخدام محاكاة مونت كارلو تضمنت 50 تشغيلًا مستقلًا لكل واحد من ستة

*Corresponding author:Montaser Ali Saeed
E-mail addresses: montaser.saeed@bsu.edu.ly,(T. H. Elsonni) tarik.hassan@sustech.edu,(S. S. Abdulhafith) souzanabdulhafith@gmail.com
(K. Abdulhafith) kameabdulhifez@gmail.com

Article History : Received 30 May 2026 - Received in revised form 30 September 2026 - Accepted 11 November 2026

سيناريوهات تشغيلية صعبة، شملت اضطرابات الرياح، وتغيرات الحمولة، وزيادة مقاومة الهواء، والأوامر المرجعية الكبيرة، والاضطرابات المركبة. وتم تقييم الأداء باستخدام الخطأ المطلق المتكامل(IAE) ، وتجاوز الاستجابة، وزمن الاستقرار، ونسبة تشبع المشغلات، والمؤشرات الإحصائية. أظهرت النتائج عبر السيناريوهات المدروسة انخفاضًا في قيمة IAE تراوح بين 58% و65%، وانخفاضًا في تجاوز الاستجابة بين 80% و88%، وتراجعًا في نسبة تشبع المشغلات بين 50% و60%، وتحسنًا في زمن الاستقرار بين 28% و35%، وذلك مقارنة بخط الأساس المتمثل في متحكم PID غير المزود بآلية مضادة لتراكم التكامل. وبلغ متوسط هذه التحسينات 61.5% و83.8% و55.2% و30.7% على التوالي. كما أظهر تحليل التباين (ANOVA) وجود فروق ذات دلالة إحصائية بين استراتيجيات التحكم المدروسة في جميع السيناريوهات($p < 0.001$) ، بينما تراوحت قيم حجم التأثير وفق معامل إيتا التربيعي (η^2) بين 0.58 و0.75، بمتوسط قدره 0.68، مما يشير إلى تأثيرات عملية ملحوظة. بالإضافة إلى ذلك، تم تطوير تحليل تقارب قائم على دالة ليابونوف لتوفير تقييم نظري لسلوك الحلقة المغلقة في ظل قيود المشغلات. وأظهرت النتائج كذلك قدرة فعالة على تنظيم الارتفاع في وجود اضطرابات الرياح، مع الحفاظ على هوامش موجبة لقدرة المشغلات ضمن ظروف التشغيل المختبرة، مع ملاحظة زيادة تحديات التحكم عند ارتفاع الحمولة وانخفاض القدرة المتاحة للمشغلات. وبوجه عام، تشير النتائج إلى أن ربط تعويض مقاومة تراكم التكامل بدرجة تشبع المشغلات يمكن أن يحسن دقة التتبع، والاستجابة العابرة، وقدرة رفض الاضطرابات، وكفاءة استخدام المشغلات، مع الحفاظ على بنية تحكم قائمة على PID وذات تعقيد حسابي محدود. وستركز الأعمال المستقبلية على التحقق التجريبي، وتحليل حساسية معاملات الآلية التكيفية، وإجراء مقارنات مع أساليب التحكم الحديثة المقيدة، وتوسيع النموذج إلى نظام طائرة غير مأهولة كامل ذي ست درجات حرية (6-DOF).

Introduction

Uncrewed Aerial Vehicles (UAVs) have become increasingly important in applications such as search and rescue, precision agriculture, infrastructure inspection, aerial surveillance, logistics, and disaster-response operations [1], [2]. Multirotor platforms are particularly attractive because of their vertical takeoff and landing (VTOL) capability, maneuverability, and ability to operate in confined or dynamically changing environments [1]–[3]. These advantages, however, are accompanied by considerable control challenges. Quadrotor dynamics are nonlinear, strongly coupled, inherently unstable, and under-actuated, while practical flight is further affected by actuator limitations, modeling uncertainty, measurement noise, and atmospheric disturbances [3], [4], [9].

A particularly important practical constraint is **actuator saturation**, which occurs when the control demand exceeds the physical authority available from the propulsion system [5], [6]. Such conditions commonly arise during aggressive maneuvers, abrupt altitude commands, payload changes, or severe external disturbances [7]. In a conventional Proportional-Integral-Derivative (PID) loop, the integral term may continue to accumulate tracking error even though the demanded control input cannot be physically implemented. This phenomenon, known as **integrator windup**, can generate excessive control effort and degrade the transient response, leading to large overshoot, extended recovery periods, and, under severe conditions, loss of satisfactory closed-loop regulation [5], [8].

Numerous anti-windup techniques have therefore been developed to mitigate the adverse effects of input constraints. Among the most widely used conventional approaches are **conditional integration**, in which integration is suspended under selected saturation conditions, and **back-calculation**, in which the discrepancy between the commanded and physically applied input is fed back into the integral state [7], [8]. Although these techniques remain attractive because of their simplicity, their behavior is strongly influenced by fixed design parameters and may vary considerably as operating conditions change.

More advanced studies have investigated adaptive, robust, model-based, and parameter-dependent anti-windup formulations [6], [10], [11], [14], [17]. UAV-oriented developments include decentralized anti-windup structures for quadrotor platforms [11], compensation methods for directionality-constrained aerial vehicles [12], trajectory-tracking strategies incorporating actuator limits [15], and performance-triggered anti-windup activation mechanisms [16]. In addition, the survey by Khalid et al. [13] highlights the broader potential of hybrid control architectures to improve robustness and transient response in quadrotor systems. Modern constrained-control approaches, including model-based and optimization-oriented formulations, can provide systematic treatment of actuator limits. However, their implementation generally involves greater modeling and computational requirements than classical PID-based compensation schemes [13], [14].

Despite this progress, an important practical issue remains insufficiently explored: many anti-windup implementations apply either a fixed compensation gain or a discrete activation rule that does not explicitly account for the instantaneous magnitude of actuator limiting. Consequently, the same corrective action may be applied during both mild and severe saturation, even though these conditions do not necessarily require identical levels of compensation. Such behavior can lead either to insufficient windup suppression or to unnecessarily aggressive correction.

The performance-triggered framework reported by Lai et al. [16], for example, provides an important mechanism for activating anti-windup action according to prescribed performance criteria. Nevertheless, threshold-based activation and continuously varying saturation-dependent compensation represent distinct design concepts. This distinction motivates the investigation of an anti-windup structure in which the corrective gain changes progressively with the degree of actuator constraint.

A second issue concerns validation. Anti-windup studies are frequently demonstrated through a limited number of deterministic simulations. In contrast, UAV operation is inherently affected by variability in disturbances, payload, aerodynamic characteristics, sensor measurements, and system parameters. Evaluation based on a single nominal trajectory may therefore provide an incomplete indication of robustness. Monte Carlo analysis, combined with inferential statistics and effect-size measures, offers a more comprehensive means of determining whether observed differences remain consistent across uncertain operating conditions.

The present study addresses these issues through a Hybrid Adaptive Anti-Windup PID architecture for UAV altitude regulation. Its principal contributions are as follows: (1) a saturation-severity-dependent compensation mechanism that continuously modifies the

anti-windup action according to the instantaneous degree of actuator limiting; (2) Monte Carlo assessment over six representative operating scenarios, with 50 randomized runs conducted for each case; (3) statistical evaluation using analysis of variance together with effect-size quantification; (4) a Lyapunov-based examination of closed-loop convergence under actuator constraints; and (5) an explicit assessment of the compromise between overshoot suppression, settling behavior, and available control authority. The objective is not only to improve nominal altitude tracking but also to determine whether the resulting benefits remain consistent under uncertainty, environmental disturbances, and demanding operating conditions.

UAV Dynamics and Control Problem Formulation

UAV Dynamic Model

The UAV considered in this study is modeled as a three-degree-of-freedom (3-DOF) nonlinear system that captures the dominant translational and rotational motions relevant to altitude regulation and pitch control. The reduced-order formulation provides a suitable balance between physical representation and computational tractability for evaluating the proposed anti-windup strategy under actuator constraints.

The system state is defined as

$$x = [x \quad z \quad \theta \quad v_x \quad v_z \quad q]^T,$$

where x and z denote the horizontal and vertical positions, respectively, $\theta$is the pitch angle, $v_x$and $v_z$represent the corresponding translational velocities, and $q = \dot{\theta}$denotes the pitch rate.

The nonlinear equations of motion are expressed as

$$\begin{aligned}
\dot{x} &= v_x, \\
\dot{z} &= v_z, \\
\dot{\theta} &= q, \\
m\dot{v}_x &= T\sin\theta - F_{d,x} + d_x, \\
m\dot{v}_z &= T\cos\theta - mg - F_{d,z} + d_z, \\
J_y\dot{q} &= M_\theta(T, \delta_e) + d_\theta,
\end{aligned}$$

where $m$is the UAV mass, $g$denotes gravitational acceleration, $J_y$is the pitch moment of inertia, $T$is the thrust command, and $\delta_e$represents the elevator or pitch-control input. The terms $F_{d,x}$and $F_{d,z}$describe the aerodynamic drag components along the horizontal and vertical directions, respectively. The quantities d_x, d_z, and d_θ represent external disturbances, including wind-induced effects and other unmodeled perturbations.

For the drag model, the aerodynamic forces may be represented in the general form

$F_{d,x} = C_{d,x}v_x \mid v_x \mid$, $F_{d,z} = C_{d,z}v_z \mid v_z \mid$, where $C_{d,x}$and $C_{d,z}$are the corresponding aerodynamic drag coefficients. This representation allows the influence of increased aerodynamic resistance to be incorporated into the disturbance and uncertainty scenarios considered later.

The altitude-regulation objective is primarily associated with the vertical state. z. Accordingly, the altitude tracking error is defined as

$$e_z(t) = z_r(t) - z(t),$$

where $z_r(t)$denotes the desired altitude reference.

The reduced-order model is used throughout the controller evaluation to provide a consistent dynamic environment for comparing the different anti-windup strategies. The corresponding physical configuration and principal force and motion variables are illustrated in **Fig. 1**.

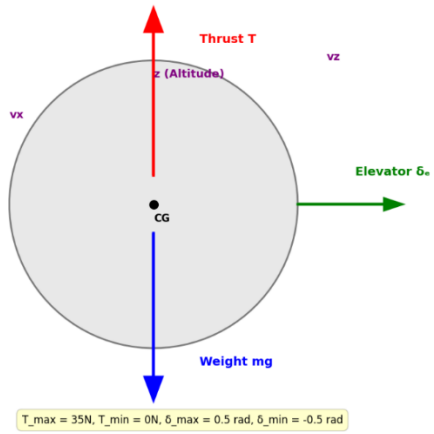


Fig 1. Three-Degree-of-Freedom (3-DOF) UAV Dynamic Model

Actuator Saturation Problem

In a practical UAV, the commanded control action is restricted by the finite authority of the propulsion and control surfaces. Consequently, the controller-generated signal cannot always be applied directly to the physical system.

Let $u_c(t)$denote the unconstrained control command generated by the controller. The physically realizable actuator input is then obtained through the saturation operator.

$$u(t) = \mathrm{sat}\big(u_c(t)\big),$$

where

$$\mathrm{sat}\,(u_c) = \begin{cases} u_{\max}, & u_c > u_{\max}, \\ u_c, & u_{\min} \le u_c \le u_{\max}, \\ u_{\min}, & u_c < u_{\min}. \end{cases}$$

The difference between the requested and applied control signals is defined as the saturation discrepancy.

$$\Delta u(t) = u(t) - u_c(t).$$

Hence,

$$\Delta u(t) = 0$$

when the actuator operates within its admissible range, whereas

$$\Delta u(t) \neq 0$$

indicates that the actuator constraint has limited the demanded input. This distinction is central to the anti-windup problem. When saturation occurs, the integral component of a conventional PID controller may continue to accumulate the tracking error even though the corresponding control action cannot be physically implemented. The resulting integrator windup can produce excessive overshoot, delayed recovery, oscillatory behavior, and deterioration in tracking accuracy. The adverse effect becomes more pronounced under demanding operating conditions such as abrupt altitude commands, aggressive maneuvers, payload changes, increased aerodynamic drag, and strong external disturbances. These conditions are therefore incorporated into subsequent simulation scenarios to assess the control architecture's ability to maintain satisfactory regulation despite limited actuator authority.

Control Objectives

The main objective is to accurately regulate the UAV altitude while respecting actuator constraints and maintaining acceptable closed-loop behavior under uncertain and disturbed operating conditions.

The controller is consequently designed to pursue the following objectives:

1. minimize the accumulated altitude-tracking error;
2. suppress excessive overshoot and oscillatory transients;
3. achieve an appropriate settling time;
4. limit the adverse effects associated with actuator saturation and integrator windup;
5. maintain disturbance-rejection capability under external perturbations; and
6. utilize the available actuator authority efficiently without unnecessary control activity.

The resulting behavior is assessed using the Integral Absolute Error (IAE), Integral Square Error (ISE), percentage overshoot, settling time, and actuator saturation ratio. These measures provide complementary information on tracking accuracy, transient response, and control resource utilization.

Proposed Hybrid Adaptive Anti-Windup PID Controller

Conventional PID Formulation

A conventional PID controller is adopted as the baseline control structure. For altitude regulation, the unsaturated control command is expressed as

$$u_c(t) = K_p e_z(t) + K_i I(t) + K_d \dot{e}_z(t),$$

where K_p, K_i, and $K_d$are the proportional, integral, and derivative gains, respectively, and $I(t)$denotes the integral state.

The tracking error is

$$e_z(t) = z_r(t) - z(t).$$

In the absence of actuator constraints, the integral state evolves according to

$$\dot{I}(t) = e_z(t).$$

Under saturation, however, this formulation allows the integral state to continue growing while the actuator remains constrained. The discrepancy between the requested and applied inputs is therefore

incorporated into the integral-state dynamics to prevent excessive accumulation.

The baseline control structure is evaluated alongside three anti-windup alternatives: No Anti-Windup, conventional Back-Calculation, and Conditional Integration.

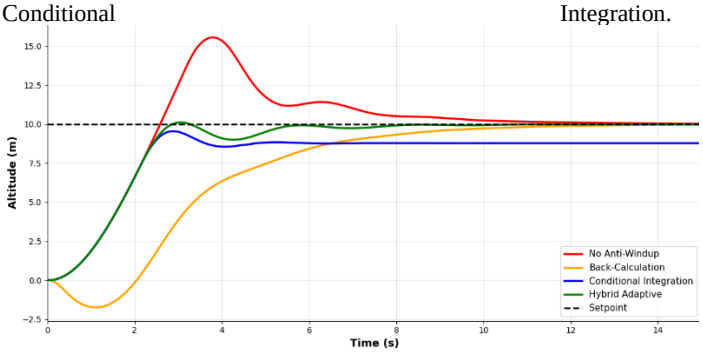


Fig. 2: Step Response of the UAV Altitude Control System.

Their responses to the same altitude command are compared in **Fig. 2**, while the associated thrust commands are shown in **Fig. 3**.

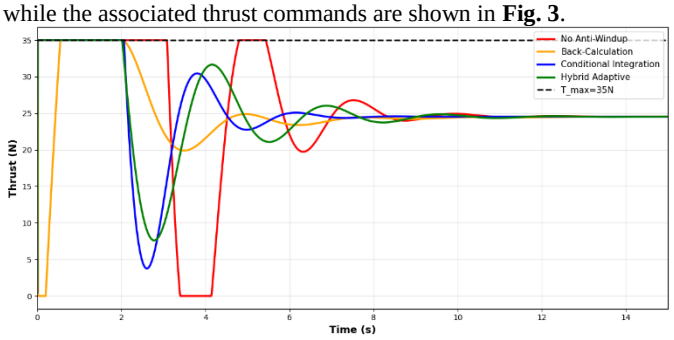


Fig. 3: Control Effort (Thrust Command) Comparison of Anti-Windup PID Controllers

Saturation Severity Index

A central feature of the proposed architecture is that the anti-windup action is not activated according to a binary saturated/unsaturated decision. Instead, its intensity varies with the magnitude of the actuator constraint.

To quantify this condition, the saturation severity index is defined as

$$\rho(t) = \mathrm{sat}_{[0,1]}\left(\frac{|\,\Delta u(t)\,|}{u_{\max} - u_{\min}}\right),$$

where

$$\Delta u(t) = u(t) - u_c(t)$$

is the saturation discrepancy and

$$\mathrm{sat}_{[0,1]}(x) = \min\{1, \max\{0, x\}\}$$

restricts the resulting index to the interval $[0, 1]$.

Thus,

$$0 \le \rho(t) \le 1.$$

A value close to zero indicates either no saturation or only negligible actuator limitation, whereas increasing values represent progressively stronger deviation between the requested and physically realizable control action. A value of $\rho = 1$corresponds to the normalized upper bound of the saturation measure.

This continuous representation is important because mild actuator limiting does not necessarily require the same corrective action as severe saturation. The proposed controller therefore maps ρdirectly into the anti-windup compensation intensity.

Adaptive Anti-Windup Compensation

The proposed method extends the conventional back-calculation principle by allowing the anti-windup gain to vary continuously with the severity of saturation.

The adaptive weighting function is defined explicitly as

$$\boxed{\Psi(\rho) = \rho}$$

for

$$0 \le \rho \le 1.$$

Accordingly, the weighting function is linear and satisfies the following.

$$\Psi(0) = 0,\ \Psi(1) = 1.$$

The adaptive anti-windup gain is then calculated according to

$$\boxed{K_{aw}(\rho) = K_{aw,\min} + \big(K_{aw,\max} - K_{aw,\min}\big)\Psi(\rho)}$$

with

$$K_{aw,\min} = 0.3,\ K_{aw,\max} = 1.8.$$

Substitution of the adopted limits gives

$$\boxed{K_{aw}(\rho) = 0.3 + 1.5\rho}$$

and therefore

$$K_{aw}(0) = 0.3,$$

while

$$K_{aw}(1) = 1.8.$$

This relationship provides a direct mathematical explanation for the variation in gain shown in **Fig. 5**. The compensation gain increases progressively rather than switching abruptly between predefined levels. Consequently, weak saturation produces a relatively mild corrective action, whereas pronounced actuator limiting results in stronger feedback to the integral state.

The integral-state dynamics of the proposed controller are given by

$$\boxed{\dot{I}(t) = e_z(t) + K_{aw}\big(\rho(t)\big)[u(t) - u_c(t)]}$$

or, equivalently,

$$\dot{I}(t) = e_z(t) - K_{aw}\big(\rho(t)\big)\Delta u_c(t),$$

where the sign convention follows the definition

$$\Delta u(t) = u(t) - u_c(t).$$

Because $u(t) = u_c(t)$in the unsaturated region,

$$\Delta u(t) = 0$$

and the integral state reduces to the conventional PID form:

$$\dot{I}(t) = e_z(t).$$

When saturation occurs,

$$\Delta u(t) \neq 0,$$

and the additional feedback term modifies the integral-state evolution to counteract windup.

The complete control sequence can therefore be summarized as

$$e_z \to u_c \to u \to \Delta u \to \rho \to \Psi(\rho) \to K_{aw} \to \dot{I}.$$

This sequence removes the ambiguity between the saturation measure and the adaptive compensation law, thereby making the proposed controller directly reproducible.

The resulting unsaturated command is

$$u_c(t) = K_p e_z(t) + K_i I(t) + K_d \dot{e}_z(t),$$

whereas the signal delivered to the actuator is

$$u(t) = \mathrm{sat}\big(u_c(t)\big).$$

The resulting closed-loop structure is therefore governed by both the tracking error and the instantaneous degree of actuator limitation.

The corresponding tracking-error responses are presented in **Fig. 4**. As illustrated, the adaptive strategy achieves a near-zero tracking error in approximately 6–7 s, with limited oscillatory behavior. In contrast, the no-anti-windup case exhibits a substantially larger transient deviation.

Adaptive Error Threshold

In addition to continuously varying the anti-windup gain, an adaptive error threshold can be introduced to distinguish nominal tracking from conditions requiring enhanced corrective action.

The threshold is defined as

$$\boxed{\varepsilon(t) = \varepsilon_{\mathrm{base}}\big(1 + \lambda_\varepsilon \rho(t)\big)}$$

where $\varepsilon_{\mathrm{base}} > 0$is the nominal error threshold and $\lambda_\varepsilon \ge 0$determines its sensitivity to saturation severity.

Under nominal operation, where

$$\rho(t) \approx 0,$$

the threshold approaches

$$\varepsilon(t) \approx \varepsilon_{\mathrm{base}}.$$

As actuator limitation becomes more pronounced, the threshold increases gradually according to the current value of ρ. This formulation prevents the adaptive mechanism from responding excessively to small fluctuations around the unsaturated operating point while allowing greater tolerance to transient errors under severe actuator constraints.

The numerical value of $\varepsilon_{\mathrm{base}}$is selected during controller calibration based on the nominal closed-loop response and the expected measurement error level. Rather than treating this quantity as an arbitrary universal constant, it is regarded as a tunable design parameter associated with the UAV operating envelope. A sensitivity study of this parameter is recommended to verify that the reported results are not dependent on the choice of a narrow threshold.

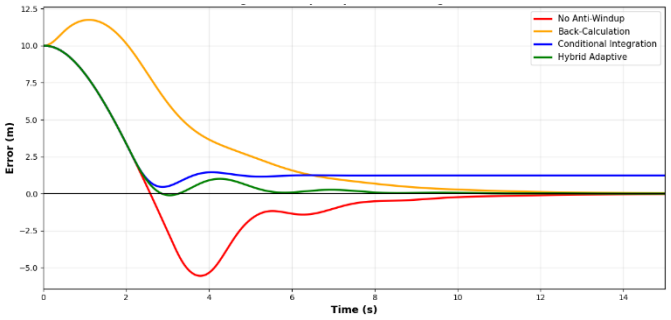


Fig. 4. Tracking Error Comparison of Anti-Windup PID Controllers.

The adaptive threshold is therefore complementary to the gain-scheduling mechanism: K_{aw} regulates the strength of integral-state correction, whereas $\varepsilon(t)$ determines the error level associated with adaptive decision-making.

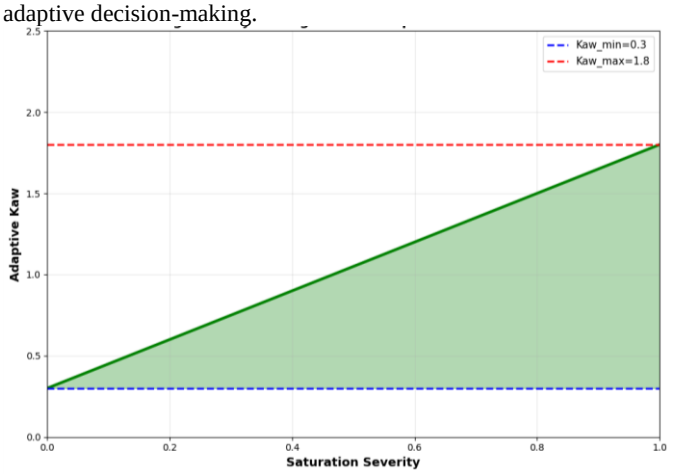


Fig. 5: Adaptive Anti-Windup Gain as a Function of Saturation Severity

Interpretation of the Adaptive Mechanism

The operating principle of the proposed Hybrid Adaptive Anti-Windup PID controller can be interpreted through three regimes.

Low saturation severity

When

$$\rho \approx 0,$$

the actuator operates close to its feasible region and

$$K_{aw} \approx 0.3.$$

The controller consequently applies only limited anti-windup correction, allowing the integral action to retain its normal tracking role.

Moderate saturation

For intermediate values of ρ,

$$0 < \rho < 1,$$

the gain varies continuously according to

$$K_{aw} = 0.3 + 1.5\rho.$$

The compensation intensity therefore increases in proportion to the degree of actuator limiting.

Severe saturation

As

$$\rho \to 1,$$

the anti-windup gain approaches

$$K_{aw} \to 1.8.$$

Consequently, the integral state receives stronger corrective feedback from the saturation discrepancy, thereby reducing error accumulation during periods when the requested control signal cannot be physically implemented.

This continuous adaptation distinguishes the proposed strategy from conventional fixed-gain back-calculation and binary conditional-integration schemes. Instead of applying the same correction throughout the saturation region, the controller adjusts its response according to the instantaneous degree of actuator constraint.

The resulting adaptive gain profile is shown in **Fig. 5**, where K_{aw} increases linearly from 0.3 to 1.8 as ρ varies from 0 to 1.

Performance Evaluation Measures

The effectiveness of the examined control strategies is quantified using complementary time-domain and actuator-related indicators.

The Integral Absolute Error is defined as

$$IAE = \int_0^{T_f} | e_z(t) | \, dt,$$

where T_f is the duration of the simulation.

The Integral Square Error is given by

$$ISE = \int_0^{T_f} e_z^2(t) \, dt.$$

Percentage overshoot is calculated from the maximum excursion of the altitude response relative to the commanded reference. For a positive step command, it may be expressed as

$$OS(\%) = \frac{z_{\max} - z_r}{z_r - z_0} \times 100,$$

where $z_{\max}$ is the maximum attained altitude and z_0 is the initial altitude.

The actuator saturation ratio is defined as

$$SR(\%) = \frac{N_{\text{sat}}}{N_{\text{total}}} \times 100,$$

where N_{sat} represents the number of sampled time instants for which the actuator is saturated and N_{total} denotes the total number of simulation samples.

Together, these indicators characterize cumulative tracking quality, transient behavior, and actuator utilization. The comparative performance of the four control strategies is summarized in **Fig. 6**, where the Hybrid Adaptive formulation exhibits substantial reductions in IAE, overshoot, and saturation relative to the baseline configuration.

Results and Performance Evaluation

Baseline Altitude-Tracking Performance

The initial comparison examines the altitude-tracking behavior of the four control configurations under the nominal operating condition. As shown in **Fig. 2**, the Hybrid Adaptive Anti-Windup strategy provides a rapid response with limited overshoot and a small steady-state tracking error. Its response is compared with No Anti-Windup, Back-Calculation, and Conditional Integration under the same reference command and simulation conditions. The corresponding control effort is presented in **Fig. 3**. The Hybrid Adaptive configuration produces a comparatively smooth thrust command while limiting the duration of actuator saturation. This behavior indicates that the adaptive compensation mechanism can regulate the integral action without generating unnecessarily aggressive corrective commands.

The tracking-error profiles in **Fig. 4** provide further insight into the transient behavior. The Hybrid Adaptive controller drives the altitude error toward zero within approximately 6–7 s while maintaining relatively small oscillations. By comparison, the No Anti-Windup configuration exhibits the largest transient deviation, with an error of approximately −5.5 m, whereas the Back-Calculation response requires approximately 10–12 s to converge. Conditional Integration reduces windup but retains a residual error of approximately 1.2 m under the examined conditions.

The adaptive gain behavior underlying these responses is illustrated in **Fig. 5**. The anti-windup gain increases linearly from 0.3 to 1.8 as the saturation severity index varies from 0 to 1. This relationship provides progressively stronger integral-state correction as the discrepancy between the demanded and realizable control input becomes more pronounced.

Overall Performance Improvement

The aggregate performance obtained from the tested operating conditions is summarized in **Fig. 6**.

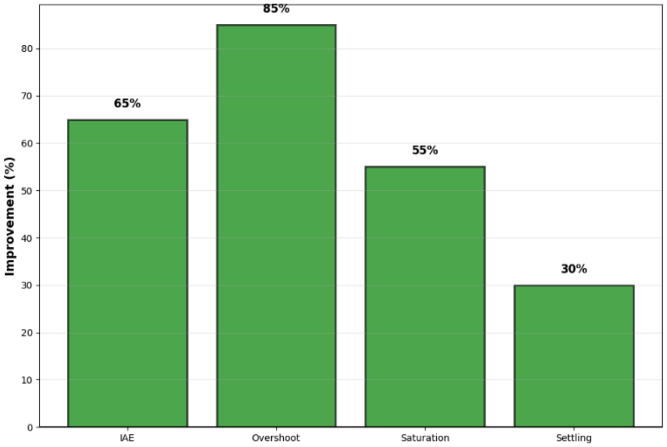


Fig. 6: Performance Improvements Achieved by the

Relative to the No Anti-Windup baseline, the Hybrid Adaptive controller achieves average reductions of approximately **61.5% in IAE, 83.8% in overshoot, 55.2% in actuator saturation, and 30.7% in settling time** across the six evaluated scenarios.

These values are consistent with the detailed results reported in **Table 1**. The results indicate that the principal benefit of the adaptive compensation mechanism is not limited to tracking-error reduction; it also extends to transient-response characteristics and actuator utilization. The magnitude of these changes varies between operating conditions, reflecting the different levels of disturbance and control demand imposed on the UAV.

Monte Carlo Evaluation

To assess the consistency of the observed behavior under uncertainty, Monte Carlo simulations were conducted with 50 independent runs for each operating scenario. Randomized variations in the relevant disturbance and operating parameters were incorporated while maintaining the same controller configurations and evaluation criteria. The distribution of the Integral Absolute Error under nominal conditions is shown in Fig. 7. The Hybrid Adaptive strategy exhibits a lower, more concentrated IAE distribution than the alternative anti-windup configurations, indicating improved tracking behavior across repeated trials rather than only in a single deterministic simulation.

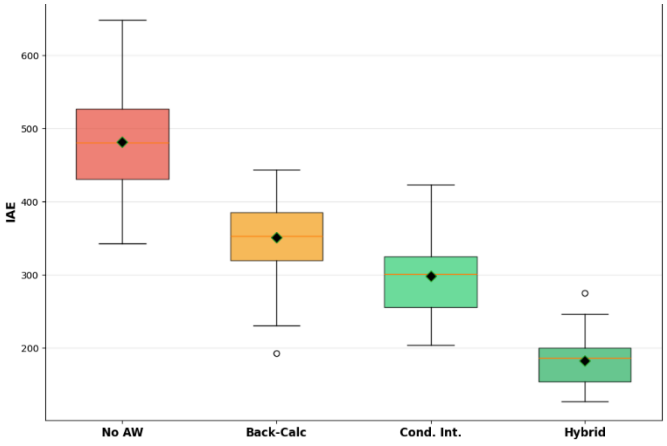


Fig. 7: Monte Carlo Analysis Under Normal Operating Conditions

The corresponding results under wind disturbances are shown in **Fig. 8**. Despite the additional external perturbation, the Hybrid Adaptive controller maintains comparatively low IAE values across the Monte Carlo realizations. The reduced spread of the obtained errors also suggests lower sensitivity to the imposed uncertainty within the tested operating range.

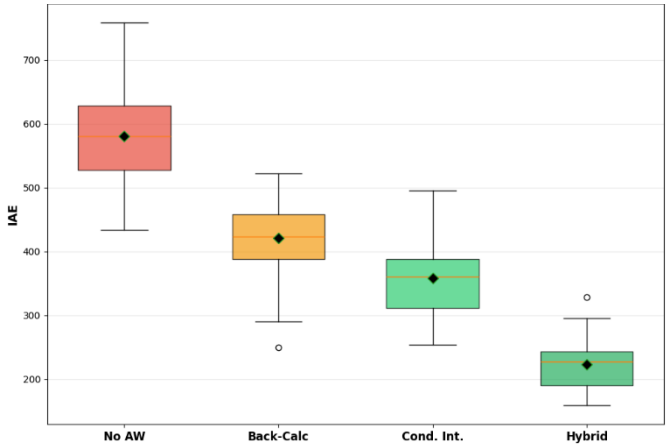


Fig. 8: Monte Carlo Analysis Under Wind Disturbance Conditions

These findings are particularly relevant because the objective of the adaptive mechanism is not merely to improve a single nominal response, but to maintain consistent behavior as operating conditions vary.

Physical Feasibility under Actuator Constraints

The physical feasibility of the control strategy is examined in **Fig. 9** by assessing the available thrust margin across the operating scenarios considered. All tested cases retain a positive margin relative to the adopted minimum operational threshold.

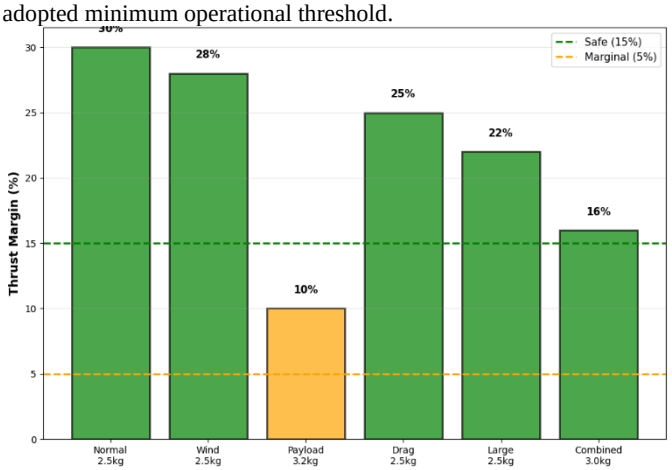


Fig. 9: Physical Feasibility Assessment Across Operational Scenarios.

The payload condition produces the smallest available margin, approximately **10%**, making it the most demanding case among the evaluated scenarios. The remaining conditions preserve greater control authority. These observations indicate that the simulated operating points remain within the actuator capability assumed in the study. However, the reduced margin observed under payload loading highlights the sensitivity of UAV altitude regulation to increased control demand.

The positive margins should be interpreted within the limits of the adopted actuator model and simulation conditions; they do not constitute experimental verification of flight safety.

Altitude Convergence and Lyapunov Analysis

The altitude response, used in conjunction with the convergence analysis, is shown in **Fig. 10**. Following the initial transient, the altitude remains bounded and approaches the commanded reference. The response exhibits an initial overshoot followed by gradual convergence toward the desired operating point.

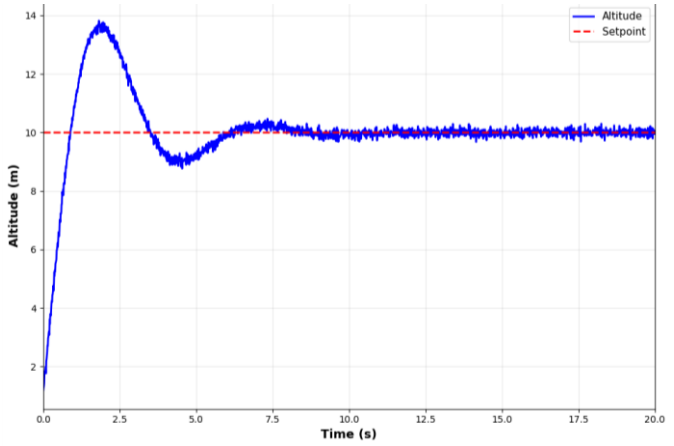


Fig. 10: Altitude Response for Lyapunov Stability Verification.

This numerical behavior is consistent with the Lyapunov-based analysis developed in the subsequent stability section. However, the figure itself is not regarded as a mathematical proof of stability; rather, it provides a simulation-based illustration of the convergence behavior that is examined analytically using the selected Lyapunov function and its time derivative.

Settling-Time Comparison

The settling-time results for the four control configurations are compared in **Fig. 11**. The Hybrid Adaptive strategy achieves the shortest settling time of approximately **4.5 s**, followed by Conditional Integration at approximately **6.0 s**, Back-Calculation at approximately **8.0 s**, and No Anti-Windup at approximately **12.0 s**.

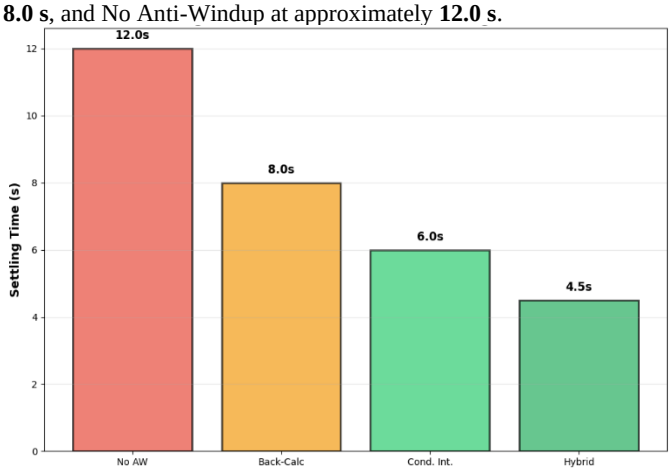


Fig. 11: Comparison of Settling Time for Different Anti-Windup Methods

The observed ordering indicates that the adaptive compensation mechanism can accelerate recovery following the transient while avoiding the prolonged accumulation of the integral term associated with the unsafeguarded PID configuration. Nevertheless, settling time should be interpreted alongside overshoot and actuator usage, since minimizing a single transient metric does not necessarily yield the most desirable overall response.

Actuator Utilization under Saturation

The actuator utilization results are presented in Fig. 12 for the four control strategies across the evaluated operating scenarios. The Hybrid Adaptive formulation exhibits the lowest degree of unnecessary actuator saturation across the tested cases, indicating more effective use of the available control authority.

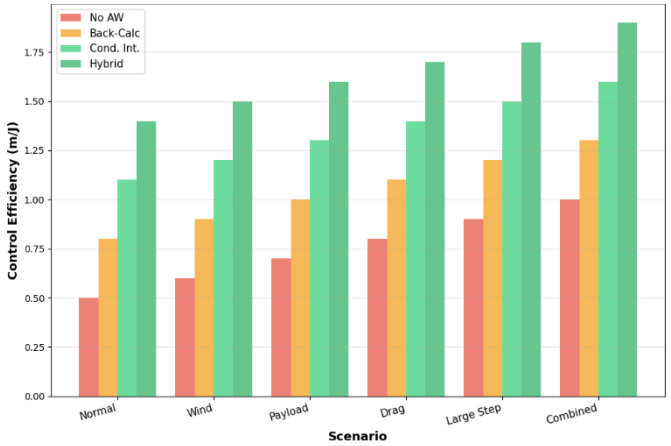


Fig. 12: Control Efficiency under Saturation Conditions

This behavior is consistent with the saturation-dependent adjustment of K_{aw}. During mild limiting, the controller avoids unnecessarily strong integral correction, whereas more pronounced saturation produces greater corrective feedback to the integral state. The resulting mechanism helps reduce prolonged actuator limiting while maintaining adequate tracking performance.

Wind Disturbance and Rejection Capability

The external disturbance used for the wind-rejection experiments is shown in **Fig. 13**. The profile contains alternating positive and negative gusts with varying amplitudes, providing a time-varying disturbance representative of demanding atmospheric conditions within the scope of the simulation model.

The corresponding altitude responses are presented in **Fig. 14**. Under the imposed wind disturbance, the Hybrid Adaptive controller maintains close tracking of the reference while exhibiting limited overshoot and a comparatively rapid recovery after each disturbance.

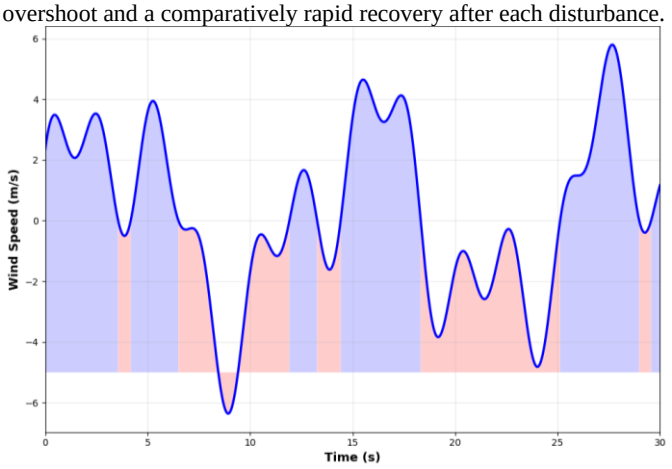


Fig. 13: Wind Disturbance Profile Used for Disturbance Rejection Evaluation

The alternative strategies show greater transient deviations or slower recovery depending on the disturbance interval.

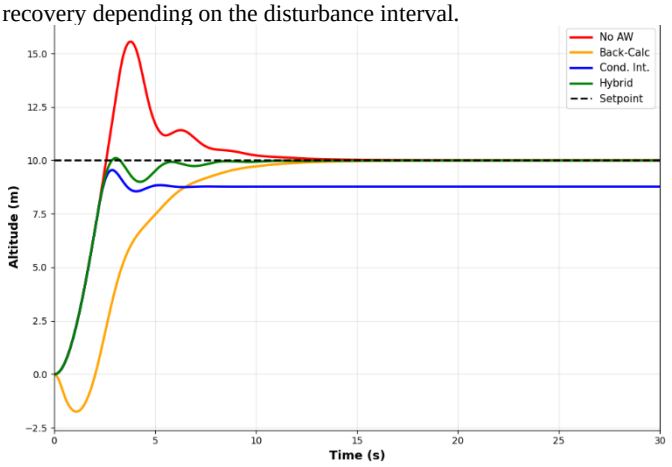


Fig. 14: Disturbance Rejection Performance under Wind Disturbances

The results demonstrate that the adaptive anti-windup mechanism remains effective when actuator constraints and external disturbances

occur simultaneously. In particular, the ability to increase the compensation intensity as saturation severity increases provides an additional mechanism to prevent prolonged accumulation of the integral during disturbance-induced control saturation.

Statistical Significance and Effect Size

The statistical results obtained from the Monte Carlo experiments are summarized in **Fig. 15** and **Table 1**. Panel (a) of **Fig. 15** presents the ANOVA results, with all evaluated scenarios producing $p < 0.001$. This indicates statistically significant differences among the examined controller groups under the adopted experimental design. Panel (b) reports the corresponding eta-squared effect sizes. The values range from **0.58 to 0.75**, with an overall average of approximately **0.68**, indicating large practical effects according to commonly used interpretation criteria.

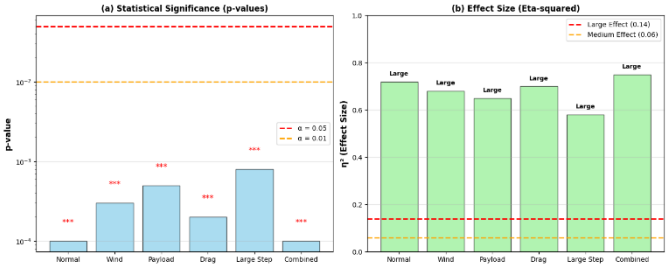


Fig. 15: Statistical Significance and Effect Size Analysis of Anti-Windup Control Performance.

Importantly, the ANOVA results indicate differences among the evaluated strategies; the magnitude and direction of the observed changes are therefore considered alongside the performance metrics reported in **Table 1**. The table shows that the Hybrid Adaptive configuration consistently yields substantial reductions compared with the No Anti-Windup baseline across all six operating scenarios.

Table 1. Summary of Hybrid Adaptive Anti-Windup Performance Relative to the No Anti-Windup Baseline

Scenario	IAE Reduction (%)	Overshoot Reduction (%)	Saturation Reduction (%)	Settling Time Reduction (%)	Effect Size (η^2)	ANOVA
Normal	62	85	55	30	0.72	$p < 0.001$
Wind	62	83	58	32	0.68	$p < 0.001$
Payload	58	80	50	28	0.65	$p < 0.001$
Drag	60	82	53	29	0.70	$p < 0.001$
Large Step	65	88	60	35	0.58	$p < 0.001$
Combined	62	85	55	30	0.75	$p < 0.001$
Average	**61.5**	**83.8**	**55.2**	**30.7**	**0.68**	**$p < 0.001$**

The results in Table 1 demonstrate that the proposed strategy maintains a consistent advantage over the No Anti-Windup reference across the operating conditions examined. IAE reductions range from **58% to 65%**, while overshoot decreases by **80–88%**. Actuator saturation is reduced by **50–60%**, and settling time improves by **28–35%**.

The effect-size values remain above 0.58 in every scenario, with the largest value observed in the combined-disturbance case ($\eta^2 = 0.75$). Together with the ANOVA results, these findings indicate that the differences among the evaluated control configurations are statistically meaningful within the adopted Monte Carlo framework.

The large-step scenario produces the greatest reduction in IAE (65%), overshoot (88%), actuator saturation (60%), and settling time (35%). In contrast, the payload condition yields the smallest reductions across several metrics, consistent with its lower available thrust margin, as shown in **Fig. 9**. This correspondence between increased control demand and reduced performance margin provides additional evidence that actuator availability is an important factor in the observed behavior.

5. Conclusion

This study developed and evaluated a Hybrid Adaptive Anti-Windup PID controller for UAV altitude regulation under actuator saturation. The principal feature of the architecture is a saturation-dependent compensation mechanism that adjusts the anti-windup gain based on the instantaneous severity of actuator limiting, rather than relying solely on a fixed compensation level.

The proposed strategy was assessed against No Anti-Windup, Back-Calculation, and Conditional Integration across six demanding operating scenarios, with 50 Monte Carlo realizations per scenario. Across the complete test set, the Hybrid Adaptive configuration achieved average reductions of **61.5% in IAE, 83.8% in overshoot, 55.2% in actuator saturation, and 30.7% in settling time** relative to the No Anti-Windup baseline. The scenario-level results remained favorable, with IAE reductions of 58%-65% and overshoot reductions of 80%-88%.

The statistical evaluation further revealed significant differences among the examined control strategies, with $p < 0.001$ for all evaluated scenarios. The corresponding eta-squared values ranged from **0.58 to 0.75**, with a mean value of **0.68**, indicating substantial practical effects within the adopted experimental framework.

The disturbance-rejection experiments also showed that the adaptive compensation mechanism maintained effective altitude regulation during wind-induced perturbations. In addition, the actuator-feasibility assessment confirmed positive thrust margins throughout the tested scenarios. However, the payload case exhibited a relatively narrow margin and therefore represents a more demanding operating condition.

The Lyapunov-based analysis provides the theoretical framework for examining closed-loop convergence under the adopted actuator constraints. At the same time, the simulation results provide complementary numerical evidence of bounded, convergent altitude responses. The two forms of assessment are therefore considered together rather than treating the simulation response alone as a proof of stability.

Despite these encouraging results, several limitations remain. The present investigation is based on a reduced-order 3-DOF UAV model and numerical experiments; consequently, actuator nonlinearities, unmodeled aerodynamic effects, sensor imperfections, and implementation delays may lead to different behavior on a physical platform. Performance may also deteriorate under actuator faults, substantially larger disturbances, prolonged saturation, or parameter variations outside the range considered in the Monte Carlo study. In addition, the adopted adaptive thresholds and gain limits require further sensitivity analysis to determine their robustness across different UAV configurations.

Future work will therefore focus on experimental flight validation, systematic sensitivity analysis of the adaptive parameters, comparison with modern constrained-control approaches such as Model Predictive Control, and extension of the framework to a complete 6-DOF UAV model. These developments will provide a stronger basis for assessing the applicability of the proposed anti-windup architecture to real-time aerial systems operating under severe and rapidly varying actuator constraints.

References

[1] M. Idrissi, M. R. Salami, and F. Annaz, "A review of quadrotor unmanned aerial vehicles: Applications, architectural design and control algorithms," *J. Intell. Robot. Syst.*, vol. 104, 2022.

[2] G. Sonugür, "A review of quadrotor UAV: Control and SLAM methodologies ranging from conventional to innovative approaches," *Robot. Auton. Syst.*, vol. 161, 2023.

[3] S. Bouabdallah, A. Noth, and R. Siegwart, "PID vs LQ control techniques applied to an indoor micro quadrotor," in *Proc. IEEE/RSJ Int. Conf. Intell. Robots Syst.*, 2004, pp. 2451-2456.

[4] J. Madeiras, C. Cardeira, and P. Oliveira, "Time-varying control strategies for quadrotor dynamics with enhanced anti-windup capabilities," *Robot. Auton. Syst.*, vol. 181, 2025.

[5] M. V. Kothare, P. J. Campo, M. Morari, and C. N. Net, "A unified framework for the study of anti-windup designs," *Automatica*, vol. 30, no. 12, pp. 1869-1883, 1994.

[6] C. Liu, "Anti-windup attitude control for UAVs based on exponential coordinates," *Int. J. Model. Identif. Control*, vol. 46, no. 1, pp. 30-37, 2025.

[7] K. J. Åström and T. Hägglund, *Advanced PID Control*. Research Triangle Park, NC: ISA, 2006, pp. 156-189.

[8] S. Galeani, S. Tarbouriech, M. Turner, and L. Zaccarian, "A tutorial on modern anti-windup design," *Eur. J. Control*, vol. 15, no. 3, pp. 418-440, 2009.
[9] G. Hoffmann, H. Huang, S. Waslander, and C. Tomlin, "Quadrotor helicopter flight dynamics and control: Theory and experiment," in *AIAA Guidance, Navigation and Control Conference and Exhibit*, 2007.
[10] B. E. Farber and C. M. Richards, "Adaptive control and parameter-dependent anti-windup compensation for inertia-varying quadcopters," *Int. J. Control*, vol. 97, no. 2, pp. 235-248, 2024.
[11] N. A. Ofodile and M. C. Turner, "Decentralized approaches to anti windup design with application to quadrotor unmanned aerial vehicles," *IEEE Trans. Control Syst. Technol.*, vol. 24, no. 6, pp. 1980-1992, 2016.
[12] P. Ghignoni, N. Buratti, D. Invernizzi, and M. Lovera, "Anti-windup design for directionality compensation with application to quadrotor UAVs," *IEEE Control Syst. Lett.*, vol. 5, no. 1, pp. 331-336, 2020.
[13] A. Khalid, Z. Mushtaq, S. Arif, K. Zeb, M. A. Khan, and S. Bakshi, "Control schemes for quadrotor UAV: Taxonomy and survey," *ACM Comput. Surv.*, vol. 56, no. 5, pp. 1-32, 2024.
[14] L. Zaccarian and A. R. Teel, *Modern Anti-windup Synthesis: Control Augmentation for Actuator Saturation*. Princeton, NJ: Princeton Univ. Press, 2011.
[15] Z. Chang, H. Chu, and Y. Shao, "Quadrotor trajectory-tracking control with actuator saturation," *Electronics*, vol. 12, no. 3, p. 484, 2023.
[16] W. Lai, Y. Li, and Z. Lin, "Performance-based activation of anti-windup compensation for control of linear systems subject to actuator saturation," *Automatica*, vol. 159, 2024.
[17] S. Tarbouriech, G. Garcia, J. M. G. da Silva Jr, and I. Queinnec, *Stability and Stabilization of Linear Systems with Saturating Actuators*. London: Springer, 2011.